Afyon Kocatepe Üniversitesi Fen ve Mühendislik Bilimleri Dergisi
Afyon Kocatepe University – Journal of Science and Engineering
https://dergipark.org.tr/tr/pub/akufemubid

Research Article
DOI: https://doi.org/10.35414/akufemubid.1469586
AKÜ FEMÜBİD 24 (2024) 051101 (1046-1052)
AKU J. Sci. Eng. 24 (2024) 051101 (1046-1052)

Impedance Matching Using Support Rod Rings in C-Band Helix TWT

*Makale Bilgisi / Article Info
Alındı/Received: 17.04.2024
Kabul/Accepted: 29.07.2024
Yayımlandı/Published: 01.10.2024

C-Bant Heliks TWT'de Destek Çubuğu Halkaları Kullanılarak Empedans Eşleştirilmesi

Ferhat BOZDUMAN[1*], Lütfi ÖKSÜZ[2]

[1] *Karabük Üniversitesi, Tıp Fakültesi, Biyofizik Anabilim Dalı, Karabük, Türkiye*
[2] *Süleyman Demirel Üniversitesi, Mühendislik ve Doğa Bilimleri Fakültesi, Fizik Bölümü, Isparta, Türkiye*

Abstract

A helical (Slow Wave Structure SWS) traveling wave tube (TWT) operating in the C bandwidth was designed using CST software. Based on modelling, TWT components were produced. Conductor support rod rings were used to matching the impedance line and provide ease of assembly. According to the modelling, the signal gain was determined as 30 dB. In addition, Time Domain Reflectometer (TDR) analyses were performed to observe the effect of mounting rings on impedance improvements with the help of software. As a result, it has been determined that the support rod rings, which have not been used before in C band helix TWT systems, positively affect the ease of assembly and impedance improvement.

Keywords: *Helix; Slow wave structure; Impedance; Traveling wave tube.*

Öz

C bant aralığında çalışan bir heliks (Yavaş Dalga Yapısı SWS) ilerleyen dalga tüpü (TWT) CST yazılımı kullanılarak tasarlanmıştır. Modellemeye dayalı olarak TWT bileşenleri üretildi. Empedans hattını eşleştirmek ve montaj kolaylığı sağlamak için iletken destek çubuk halkaları kullanıldı. Modellemeye göre sinyal kazancı 30 dB olarak belirlendi. Ayrıca yazılım yardımı ile montaj halkalarının empedans iyileştirmelerine etkisini gözlemlemek için Zaman Tanım Alanlı Reflektometre (TDR) analizleri yapılmıştır. Sonuç olarak C bant sarmal TWT sistemlerinde daha önce kullanılmamış olan destek çubuk halkalarının montaj kolaylığını ve empedans iyileştirmesini olumlu yönde etkilediği tespit edilmiştir.

Anahtar Kelimeler*: Heliks; Yavaş dalga yapısı; Empedans; İlerleyen dalga tüpü.*

1. Introduction

Microwave tubes are vacuum electronic devices that produce radio transmitters in the microwave frequency range. The millimeter wave frequency region is part of the microwave range and is generally considered to be approximately 30 GHz to 300 GHz (Gilmour 2020). The field of vacuum electronics devices, especially in the millimeter-wave range, is currently undergoing rapid evolution, transitioning from traditional microwave helix traveling-wave tubes (TWTs) to novel designs created to address the fabrication challenges posed by the shorter wavelengths in millimeter waves (Paoloni *et al.* 2021). Unlike other vacuum electronic tubes, TWTs are advantageous because they have wider band gaps (Whitaker 2001). Since TWTs have lower noise values, their use has become more widespread (Peebles 1998).

A proven technique for amplifying a specific electromagnetic wave involves passing the wave through a periodic structure and co-propagating it alongside a linear DC electron beam. To simplify matters, this interaction between the beam and circuit takes place within a vacuum. In this arrangement, the traveling wave acquires energy at the cost of the kinetic energy of the electron beam. This ongoing interaction and subsequent amplification of the electromagnetic wave persist over a specific distance, which corresponds to the length of the interaction region in the Traveling Wave Tube (TWT), until the amplified wave is extracted at the output (Wong *et al.* 2020).

As a power output comparison, in low-power TWTs, it is sufficient to use a periodic magnet system to focus the electron beam (Lakshminarasimhan *et al.* 2011). TWTs perform signal amplification based on the electron beam–wave interaction mechanism (Santos *et al.* 2011). Under normal conditions, RF waves travel at the speed of light because they are electromagnetic waves. However, since the distance they travel in the slow wave structure system is long, they have slow group velocities (Edgecombe 1993). In helical TWTs, dielectric materials electrically isolate the slow wave structure with a metallic vacuum envelope. These materials are in the form of rods with different geometric shapes. This also simplifies the

*Sorumlu Yazar/Corresponding Author: Ferhat Bozduman e-posta/e-mail: ferhatbozduman@karabuk.edu.tr

fabrication of the device (Harper and Puri 1986). Helical TWTs generally use three support rods. They are positioned at an angle of 120^0 to each other. We positioned the support rods at a 120^0 angle between them during the assembly phase. Rectangular or cylindrical structures are generally used as geometric shapes in support bars. We preferred cylindrical support rods when making our design. The helix is usually made of tungsten and molybdenum wires (Gilmour 2020). We used tungsten wire to create SWS in sizes suitable for our design. The thermal resistance of these wires is quite high. But conductivity values are limited. To eliminate this limitation, coating is applied on the material surface. We coated the surface of the wire with copper to ensure high surface conductivity.

With this method, losses on the helical surface of the RF signal are minimized. At the same time, the thermal resistance formed between the support rods and the spiral decreases. The dispersion characteristics of a helical structure can be altered by incorporating longitudinal blades between the support rods. The blade tips establish the radial boundary for the electric field, while the outer shield confines the magnetic fields. Consequently, these blades illustrate the impact of the helical slow-wave structure on dispersion and Pierce impedance (Carter 2018). In TWT systems, valves are placed in the gaps between the support rods to prevent dispersion and ensure operation in different frequency ranges. These valves are known as anisotropic loading elements. These elements are generally propeller-shaped and T-shaped (Putz and Cascone 1979). We did not use the valve structure directly in our system, but instead used the rings that hold the support rods together. These rings indirectly serve as valves. Thanks to the rings, capacitance control is provided as in an LC circuit.

Since our system was designed for low power conditions, we used SMA-type connectors in the connection ports. We produced the connectors we use ourselves. As a result, the impedance transitions at the input and output of these TWTs must match the wide variation in helix impedance. It should also be taken into account that impedance matching is important in high frequency devices. In order for signal amplification to occur efficiently, impedance matching must be at the maximum level in the SWS structure, including connection connectors.

This work discusses the use of support rod rings to matching the impedance characteristics of a C Band helical traveling wave tube (TWT). We argue that by adding these rings, the impedance mismatch between the coil and the collector can be reduced, resulting in improved performance. One important similarity between this study and previous research is the focus on impedance matching. Both studies aim to minimize reflections within the TWT and maximize power transfer. However, while previous research has primarily focused on tuning parameters such as helix spacing or collector diameter, this study presents a new approach using support rod rings. In terms of differences, this study specifically focuses on C Band helical TWTs, while previous studies have investigated various frequency bands. Additionally, although previous studies were mostly based on simulations or theoretical analysis, this paper presents experimental results to validate the proposed methods. Overall, this study provides valuable information regarding the matching of impedance characteristics in C Band helical TWTs.

By presenting support rod rings as an innovative solution, it offers a promising approach to improve device performance. Further research may reveal the applicability of this method in different frequency bands and its potential impact on other TWT parameters.

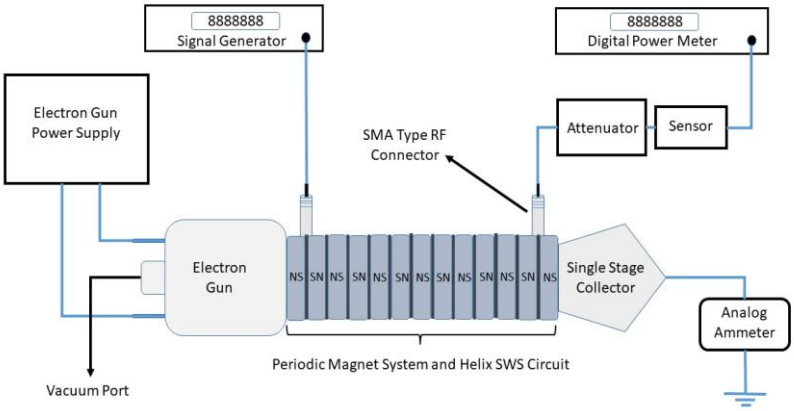

Fig. 1. Diagram of the experimental setup.

2. Materials and Methods

First of all, microwave and particle studio modules and a slow wave structure suitable for the C band range were designed using CST software. Figure 1 shows the setup diagram of the working mechanism. Then, an electron beam was created with the particle studio module according to our electron gun parameters. Figure 2 shows the modeling of an electron beam with an acceleration potential of -3kV using CST software in a computer environment with the help of permanent magnets. In the simulation, the electron beam's current is 30 mA. The graphic accelerator technique was used to get the simulation results quickly. The experimental procedure stage used A helical type helix as the slow wave structure. High-purity molybdenum wire with a diameter of 0.25 mm was chosen as the material. With the help of the coil winding machine, the helix structure was wound on the stainless steel (SS304) guide at the determined circuit length and period range. ACME AE-X model spring coiling device was used in Figure 3 to create the coil.

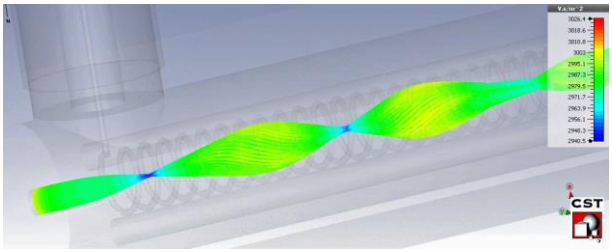

Fig. 2. Formation of the electron beam with CST.

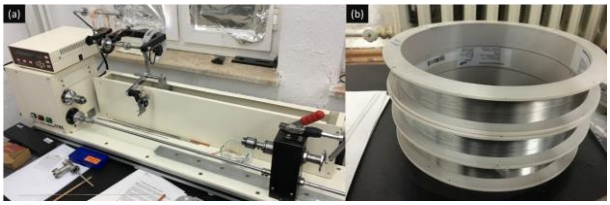

Fig. 3. ACME AE-X Coil winding machine and molybdenum coil. (a) Coil machine, (b) Molybdenum coil.

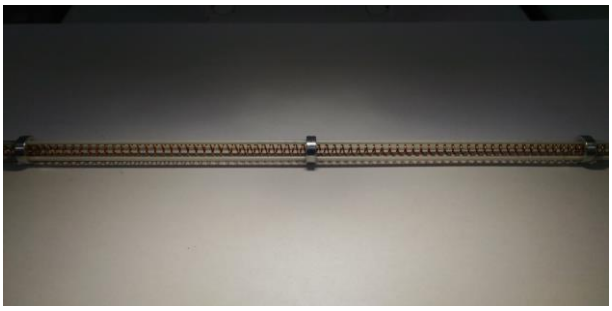

Fig. 4. Molybdenum helix coated with copper film.

In order to increase the conductivity value of the formed helix, its surface was homogeneously coated with a copper film on the turntable by using the DC magnetron sputtering technique at low pressure. Ceramic (Al_2O_3) was used as a support rod. For the support rods to contact the helix surface without gaps and smoothly, hollow rings of aluminum material were designed using CNC. At the same time, these hollow rings play a significant role in impedance matching because these rings provide an easy and trouble-free assembly of the outer sheath and SWS circuit.

Figure 4 shows the helical structure and the assembled ceramic support rods and rings. This setup is also a slow-wave RF circuit, which is the essential component of the TWT system.

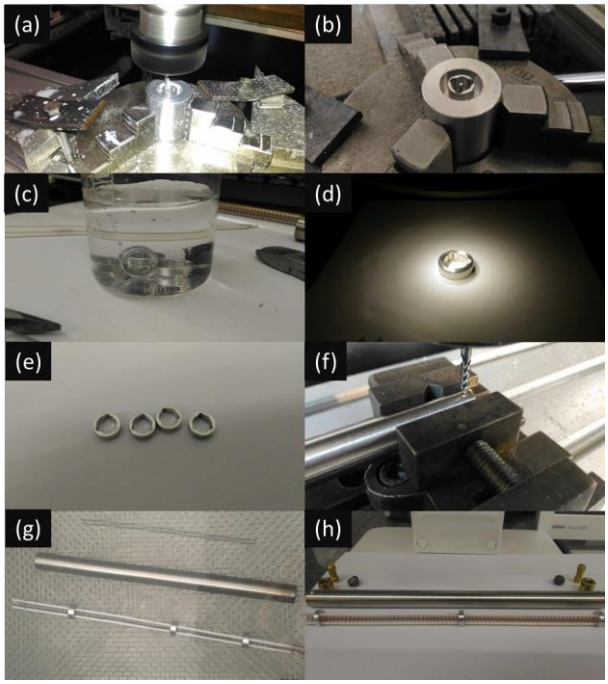

Fig. 5. Production steps of the support ring used to keep the ceramic support rods together and place them in the vacuum sleeve. (a) Ring machining, (b) Ring cutting, (c) (d) (e) Ring cleaning, (f) Rf port preparing, (g) Total system cleaning, (h) Total system assembly.

After the rings produced in Figure 5, ceramic support rods and helix were cleaned with the help of an ultrasonic bath, and assembly processes were carried out. A welded 1mm thick, 12 mm outer diameter, and 20 cm long pipe made of SS304 material was used as the vacuum sheath. SMA connector made of brass material for RF input and output. The dielectric part of the connector was formed using Teflon (PTFE) material. The created SMA-type RF connector was assembled to the metal vacuum sheath with a screw system. Ring magnets with ALNICO structure were used to create the periodic magnet system.

The dimensions of the magnets were determined as 13 mm inner diameter, 30 mm outer diameter, and 10 mm thickness. Iron rings were used to hold equimolar magnets together. The magnets are drilled to the outer diameter of the RF connectors so that the magnets can be

easily mounted between the SMA connectors. With this method, the assembly operations were carried out.

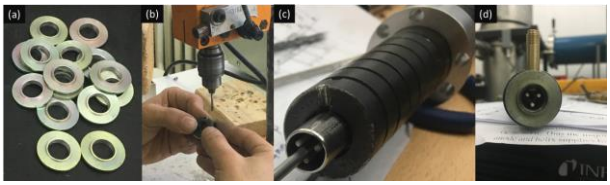

Fig. 6. Production of periodic magnet system and opening of SMA connector slots using Alnico ring magnets. (a) pole pieces, (b) machining, (c) magnets assembly, (d) RF connector assembly.

The electron gun was connected to the vacuum environment with the help of the CF40 port. Solid glass rods and aluminum rings linearly attached and aligned the periodic magnet system with the electron gun and collector. A multi-port vacuum tank with a Pyrex lantern was used as the vacuum chamber. To reduce the system's pressure to ultra-high vacuum (UHV), a double-stage oily mechanical pump and a turbo-molecular high vacuum pump were used. A convector and hot cathode ionization sensors were used to measure system pressure. Before starting the experiment, the system pressure was reduced from 760 Torr, which is atmospheric pressure, to $3.5X10^{-8}$ Torr. Our descent to ultra-high vacuum levels aims to prevent cathode poisoning.

Because oxygen (O_2), carbon monoxide (CO), carbon dioxide (CO_2), and water vapor (H_2O) in the environment at high-pressure levels will react with the heated cathode and cause poisoning of the cathode. This will reduce the emission performance of the cathode. In order to observe that the electron beam in the system is successfully focused and reaches the collector without hitting the helix surface, a serial analog ammeter is connected to the collector part via the ground. With this method, the current of the electron beam reaching the collector was measured. No signal was applied to the RF circuit while measuring. Collector with the value of the emission current indicator on the power supply screen of the electron gun. The value of the electron current reaching the surface was compared. It was observed that the results were in agreement with each other. This result is an output that the electron beam is successfully focused and passed through the helical structure without impact. Figure 7 shows the excitation of the phosphor screen used to observe the electron beam formed by the electron gun. Thanks to this method, information about the pattern and trace size of the electron beam was obtained.

Necessary vacuum conditions were provided by using a double-stage mechanical pump and turbomolecular vacuum pumps for stable operation of the electron gun. The electron gun was started after the vacuum value reached 10^{-8} Torr levels. Then, the acceleration voltage and anode voltage values were applied at the required parameters to obtain the required electron beam current. Then, the accelerating voltage was turned off, and the electron beam was cut off. In the next step, a continuous wave mode (CW) sine wave signal with a frequency of 4.93GHz and a power of 11.7 dBm, which is considered as the C band, was applied to the SMA input port of the RF circuit, which is close to the electron gun, with the help of a signal generator.

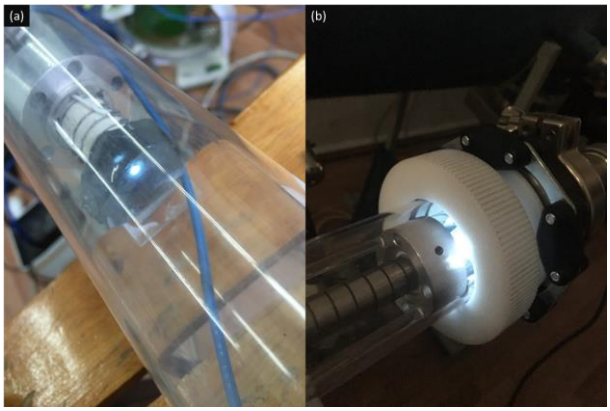

Fig. 7. Observation of the electron beam using a phosphor screen. (a) Electron beam observing, (b) Electron beam focusing.

Attenuators have been added to the output port of the RF circuit to prevent damage to the power meter and to measure the output power. Losses in cables and connection connectors have been detected. A loss of approximately 17 dB was observed in the cable and connection connectors. A 60 dB attenuator was connected as an attenuation element. While the pulse generator was on, the power meter read a signal of approximately -65 dBm from the output port. Thus, we have determined how much of a signal will be strengthened in the system. In Figure 8, the comparison of the RF power values read when the electron beam of the power meter is closed and the electron beam is open is given.

Fig. 8. Agilent E4418B model power meter used to measure the signal strength of the RF output port. (a) Electron beam off, (b) Electron beam on.

An RF signal at a power level of approximately -65 dBm was observed when an RF signal was on the power meter screen and the electron beam was turned off. At the same

time, the system had an RF signal; an approximately -35 dBm RF signal was observed when the electron beam was applied. It was determined that a signal output of approximately 30 dBm was obtained when the difference was taken, and the attenuation values in the connectors and cables in the system were added. If this value is expressed in watts, when we compare, we can say that the signal power entering the TWT system has been increased from 15 mW to 1 W. As a result, signal amplification was successfully performed. In order to achieve higher power levels, impedance-matching units must be placed at the output port of the TWT system. Because the work is done at high frequencies, there is a reflection of the power, and this causes signal losses.

3. Results and Discussions

Table 1 gives the experimental parameters of the TWT system established in the laboratory environment. These parameters were also used in the CST software. With this method, the experimental results and simulation results were compared.

Table 1. Experimental Parameters and Results of The TWT System Established in The Laboratory

Parameter	Value
Acceleration Voltage (kV)	-3
Current of Electron Beam (mA)	30
Slow Wave Circuit Length (cm)	18
Helix Diameter (mm)	3,2
Helix Pitch Interval (mm)	1,3
Thickness of Helix Wire (mm)	0,25
Number of Helix Rounds	75
Thickness of Support Rods (mm)	1,6
Input Signal Frequency (GHz)	4,93
Input Signal Power (dBm)	11,7
Output Signal Power (dBm)	30

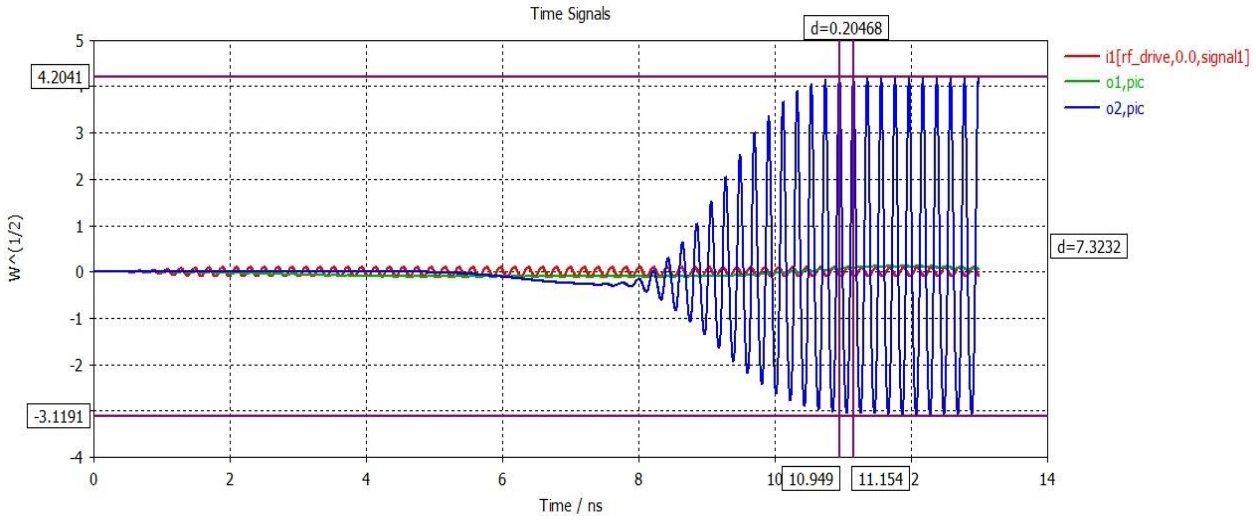

Fig. 9. Observation of signal amplification using CST software

The simulation was carried out using the TWT parameters entered in the computer environment in Figure 9. Experimental parameters and simulation parameters have the same values. As a result, the signal entered as ten mW in the simulation experiment was taken as 1 W. In the experimental result, the signal entered as 15 mW increased to 1 W. The reason for this difference is the losses and impedance mismatches in the connectors. Because there is no impedance-matching unit in the power output port of the TWT system. During the experiment, it was observed that when the RF circuit was driven at higher powers, the output signal did not change for a certain time but dropped. This is due to the formation of saturation. Because the RF circuit saturates above a particular signal strength, in the experimental setup we have set up, attenuating coating material was not used in the centers of the insulating support rods. Electron guns with attenuator coating and higher electron current must be used to achieve higher power outputs. The importance of the collector plays a significant role in the system. Because the electrons, which transfer some of their energy to the RF wave, hit the collector, and their movement ends. This event ensures that the TWT circuit continues in a closed loop. This is also important for the energy efficiency of the system. A single-stage collector was used in our experimental system. The earth connection is made as collector feed. In modern collectors, on the other hand, multistage collectors, which are less negative than the electron beam potential, are used.

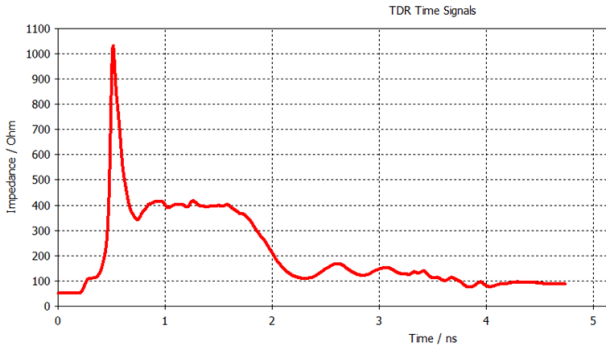

Fig. 10. Performing TDR analysis using CST software.

TDR analysis of the TWT system we designed using CST software in the computer environment in Figure 10 has been made. With this analysis, the time-dependent examination of the impedance characteristic of the transmission line was carried out. As seen in the graph, a load peak occurs. This causes an impedance mismatch in the transmission line. In this design, there are no rings to which the ceramic support rods are attached. In a subsequent TDR analysis, we used ceramic support rods and aluminum rings we designed in the laboratory environment. In this analysis, there are no peaks that disrupt the impedance characteristic. For this reason, the impedance transition of the transmission line is provided without any problems. Figure 11 shows the TDR analysis performed with the ring design.

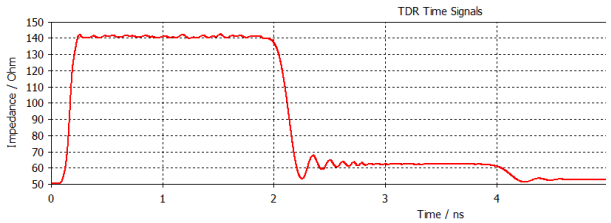

Fig. 11. TDR analysis with ring design.

The 15 mW and 4.93 GHz RF signal applied to the input port of the TWT system was measured as 1 W at the output port. A TWT that can operate in the C band and gain approximately 30 dB has been produced. Signal losses in the system have occurred in cable and connector connections. In addition, reflections caused by the absence of an impedance-matching unit at the output port affected our small-scale results. One of the most important factors was machining parts on the micron scale during manufacturing and assembly. In addition, the experimental results and the simulation results must match.

4. Conclusions

As a result of this study shows how the assembly steps are performed with impedance matching for the helix C band space TWT with 1 W output power. In addition, vacuum tube design was carried out in allowable dimensions using CST-MWS simulation software. Thus, the simulation results were adapted to the experimental study.

Declaration of Ethical Standards

The authors declare that they comply with all ethical standards.

Credit Authorship Contribution Statement

Author-1: Sources, Research, Experiment, Writing - original draft Visualization, Writing - original draft

Author-2: Research, Formal analysis, Verification

Declaration of Competing Interest

The authors have no conflicts of interest to declare regarding the content of this article.

Data Availability

All data generated or analyzed during this study are included in this published paper.

Acknowledgement

This work was supported by Tubitak project number 1140075. We would also like to thank PlazmaTek company, which hosts experimental and theoretical studies, for their support.

5. References

Carter, R.G., 2018. Microwave and RF Vacuum Electronic Power Sources. ed. S.C. Cripps, Press, UK: Cambridge University, 508-509.

Deng, W.K., Hu, Y.L., Li, G.B., Yang, Z.H., Li, B. and Huang, T., 2023. Performance Improvement of Helix Traveling- Wave Tubes Based on Multiobjective Optimization Technique. *IEEE Transactions Electron Devices,* **70,** 2840-2845. https://doi.org/10.1109/TED.2022.3207711

Edgecombe, C., 1993. Gyrotron Oscillators. ed. C J Edgecombe, London: CRC Press, 40-41.

Gilmour, A.S., 2020. Microwave and millimeter-wave vacuum electron devices: inductive output tubes, klystrons, traveling-wave tubes, magnetrons, crossed-field amplifiers, and gyrotrons. ed. J Gomes, Boston: Artech House, 357-358.

Harper, R. and Puri, M.P., 1986. Heat transfer and power capabilities of EFH helix TWT's. *International Electron Devices Meeting,* 498-500.

Lakshminarasimhan, R., Venkatesh, V., Ravindra, M. and Nanjundaswamy, T.S., 2011. Development of 60 W C-Band TWT for space. *IEEE International Vacuum Electronics Conference (IVEC),* (Bangalore, Karnataka, India: IEEE), 77-78. https://doi.org/10.1109/IVEC.2011.5746883

Paoloni, C., Gamzina, D., Letizia, R., Zheng, Y. and Luhmann, N.C., 2021. Millimeter wave traveling wave tubes for the 21st Century. *Journal of Electromagnetic*

Waves and Applications, **35,** 567-603. https://doi.org/10.1080/09205071.2020.1848643

Peebles, P.Z., 1998. Radar Principles. New York: Wiley, 1.

Prakash, D.J., Dwyer, M.M., Argudo, M.M., Debasu, M.L., Dibaji, H., Lagally, M.G., Van Der Weide, D.W. and Cavallo, F., 2021. Self-Winding Helices as Slow-Wave Structures for Sub-Millimeter Traveling-Wave Tubes. *ACS Nano,* **15**, 1229-1239. https://doi.org/10.1021/acsnano.0c08296

Putz, J.L. and Cascone, M.J., 1979. Effective Use of Dispersion Shaping in Broadband Helix TWT Circuits. *International Electron Devices Meeting*, 422-424.

Santos, G.M.S., Xavier, C.C. and Motta, C.C., 2011. A Study of a PPM Focusing System for a C Band Power TWT. *International Conference on Microwave and Optoelectronics,* Natal, Brazil: IEEE, 941-945. https://doi.org/10.1109/IMOC.2011.6169399

Trubetskov, D.I. and Vdovina, G.M., 2020. Traveling wave tubes: a history of people and fates. *Physics-Uspekhi,***63,**503. https://doi.org/10.3367/ufne.2019.12.038707

Whitaker, J.C., 2001. The resource handbook of electronics. ed. J C Whitaker, Boca Raton, Fla: CRC Press, 45-46.

Wong, P., Zhang, P. and Luginsland, J., 2020. Recent theory of traveling-wave tubes: a tutorial-review. *Plasma Research Express,* **2**, 1-19. https://doi.org/10.1088/2516-1067/ab9730

Wu, G., Yin, H., Xu, Z., Yang, R., Lei, X., Li, Q., Yue, L., Xu, J., Zhao, G., Park, G.S. and Wei, Y., 2020. Design and Experimental Measurement of Input and Output Couplers for a 6–18-GHz High-Power Helix Traveling Wave Tube Amplifier. *IEEE Transactions Electron Devices,***67,**1826-1831. https://doi.org/10.1109/TED.2020.2975645

Wu, G., Yin, H., Xu, Z., Yang, R., Lei, X., Li, Q., Fang, S., Yue, L., Xu, J., Zhao, G., Wang, W. and Wei, Y., 2020. Design of a Pseudoperiodic Slow Wave Structure for a 6-kW-Level Broadband Helix Traveling-Wave Tube Amplifier. *IEEE Transactions Plasma Science,* **48,** 1910-1916. https://doi.org/10.1109/TPS.2020.2971149